Organic & Biomolecular Chemistry

Cite this: *Org. Biomol. Chem.*, 2011, **9**, 1600

www.rsc.org/obc

PAPER

Synthesis of star-shaped monodisperse oligo(9,9-di-n-octylfluorene-2,7-vinylene)s functionalized truxenes with two-photon absorption properties†

Huipeng Zhou,[a] Xin Zhao,[a] Tianhao Huang,[b] Ran Lu,*[a] Hanzhuang Zhang,[b] Xiaohui Qi,[b] Pengchong Xue,[a] Xingliang Liu[a] and Xiaofei Zhang[a]

Received 30th September 2010, Accepted 23rd November 2010
DOI: 10.1039/c0ob00803f

A series of new star-shaped monodisperse conjugated truxene derivatives bearing oligo(fluorene-vinylene) arms (**Tr-OFV*n***, n = 1, 2, 3, 4) have been synthesized. It is found that the conjugation of the oligomers can be extended with prolonging the arms. Notably, the branched oligomers **Tr-OFV*n*** without strong donor and acceptor units exhibit two-photon absorption properties, and the two-photon absorption cross sections (δ_{max}) increase with increasing the number of fluorene-vinylene units in the arms. The maximum value of δ_{max} reaches 8073 GM for compound **Tr-OFV4**, which made it one of the most competitive compounds with enhanced TPA cross section. It provides a new platform for exploiting strong TPA compounds, in which the extended π-conjugated systems are involved in the absence of strong donor and acceptor units.

Introduction

Materials exhibiting large two-photon absorption (TPA) cross sections have attracted intense interest due to their interesting frequency up-conversion mechanism and potential applications in two-photon fluorescence imaging,[1] three-dimensional optical data storage,[2] up-converted lasing,[3] photodynamic therapy,[4] and optical power limiting,[5] *etc.* To date, a great deal of effort has been devoted to exploring strong TPA compounds, and the development in understanding the structure–TPA-cross section relationship reveals that TPA cross section is related to many factors, including the donor–acceptor strength, conjugation length, and the planarity of the π-center.[6] For instance, it has been found that π-conjugated motifs with strong electron donor (D) and acceptor (A) groups, such as symmetrical (D–π–D or A–π–A) or asymmetrical (D–π–A) systems, favor for the nonlinear absorption. However, reports that focus on the conjugated system, without strong donor and acceptor units, showing high TPA cross section are limited. In addition, another strategy toward the enhancement of TPA has been employed with the use of branched chromophores where collections of TPA-active subunits can extend into multi-dimensions.[7] Among a variety of TPA compounds, fluorene, biphenyl, and styryl groups are usually used as the mobile π-electron bridge, and the most attractive π-centers focused on pyrene, benzene, biphenyl, fluorene, dithieniothiophene, and dihydrophenathrene moieties, *etc.*[8] Thus, fluorene is frequently employed as an efficient building block for the construction of the chromophores with high two-photon absorptivities. Furthermore, a near-planar and highly fused structure, truxene, contains three fluorenes sharing a central benzene ring and is facilely functionalized in three directions in space.[9] With these in mind, a series of new star-shaped conjugated oligomers of truxene-cored oligo(fluorene-vinylene)s **Tr-OFV*n*** (n = 1, 2, 3, 4) are synthesized (Chart 1), because the monodisperse conjugated oligomers possess well-defined and uniform molecular structures as well as

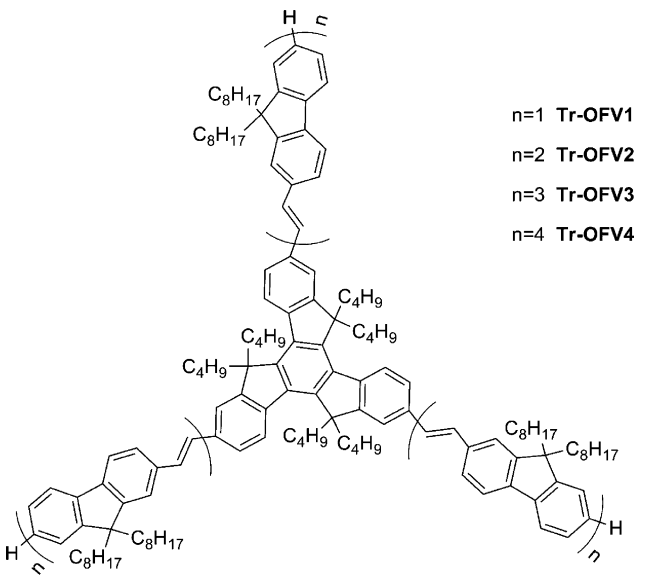

Chart 1 The molecular structures of the star-shaped molecules **Tr-OFV*n***.

[a]*State Key Laboratory of Supramolecular Structure and Materials, College of Chemistry, Jilin University, Changchun 130012, P. R. China. E-mail: luran@mail.jlu.edu.cn; Fax: +86-431-88923907; Tel: +86-431-88499179*
[b]*College of Physics, Jilin University, Changchun 130012, P. R. China*

† Electronic supplementary information (ESI) available: Cyclic voltammetry diagrams; UV-vis absorption and fluorescence spectra, two-photon excitation spectra, two-photon-induced fluorescence spectra; ^{1}H NMR, ^{13}C NMR, and MALDI/TOF MS spectra of new compounds. See DOI: 10.1039/c0ob00803f

superior chemical purity, which makes them suitable for systematic investigation of structure–property relationships.[10] Although a number of star-shaped macromolecules based on oligofluorenes cored by benzene,[11] porphyrin,[12] triazatruxene,[13] pyrene,[14] and truxenes have been synthesized,[15] the TPA properties have not been reported. Notably, no strong donor and acceptor units are involved in the obtained oligo(fluorene-vinylene)s functionalized truxenes **Tr-OFV*n***, but the conjugated oligomers still exhibit strong TPA activity. It is found that the two-photon absorption cross sections (δ_{max}) increase with prolonging the arms in the star-shaped macromolecules, and the maximal TPA cross section (δ_{max}) reaches 8073 GM, which is one of the highest δ_{max} values reported. Herein, we have provided a new platform for exploiting strong TPA compounds, in which the extended π-conjugated systems are involved in the absence of strong donor and acceptor units.

Results and discussion

Synthesis and characterizations

The synthetic strategy for **Tr-OFV*n*** (n = 1, 2, 3, 4) was following the approach exploited by Skabara and co-workers,[15] and the synthetic routes for monodisperse oligo(9,9-di-n-octylfluorene-2,7-vinylene)s functionalized truxenes **Tr-OFV*n*** are sketched in Schemes 1 and 2. The precursors of oligo(9,9-di-n-octylfluorene-2,7-vinylene)s with terminal vinylene groups ***E*-OFV*n*** (n = 1, 2, 3, 4) were first prepared by alternate Heck and Wittig reactions.[16] For example, ***E*-OFV1** was obtained through Wittig reaction between methyltriphenylphosphoniumiodine and 2-formyl-9,9-di-n-octylfluorene (**1**), which was synthesized according to the reported method[12] in a yield of 95%. Then, compound **4** was readily obtained from ***E*-OFV1** and 2-bromo-7-formyl-9,9-di-n-octylfluorene (**3**), which was an important intermediate for extending the fluorene units in ***E*-OFV*n*** and prepared in accordance with the literature,[12] catalyzed by $Pd(OAc)_2$ in DMF at 110 °C for 10 h *via* Heck reaction in a yield of 78%. The Wittig reaction between compound **4** and methyltriphenylphosphoniumiodine could afford ***E*-OFV2** in a yield of 85%. Accordingly, by using alternate Heck reaction and Wittig reactions,[17] we gained ***E*-OFV3** and ***E*-OFV4** in moderate yields. Meanwhile, 5,5,10,10,15,15-hexabutyl-2,7,12-tribromotruxene (**9**) was synthesized according to the method reported in ref. 18. For instance, truxene (**7**) was easily translated into 5,5,10,10,15,15-hexabutyl-truxene (**8**) *via*

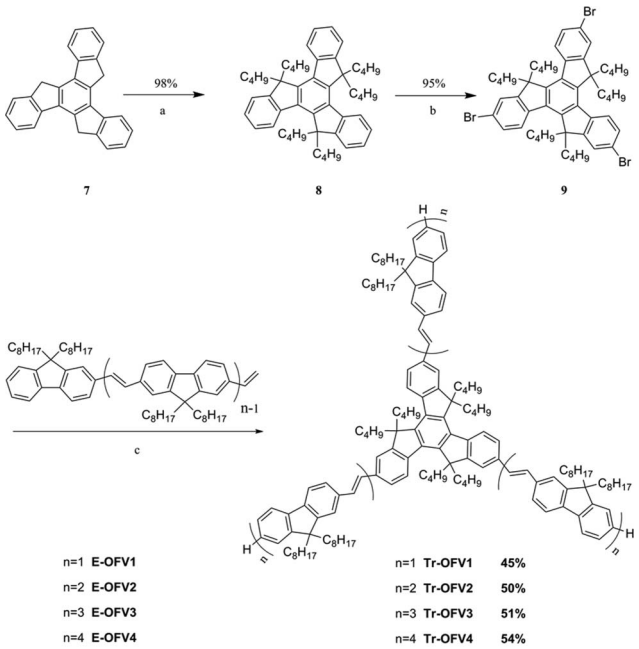

(a) 1) n-BuLi, THF, -78 °C to rt; 2) n-C_4H_9Br, -78 °C to rt; (b) Br_2, $FeCl_3$, $CHCl_3$; (c) $Pd(OAC)_2$, K_2CO_3, DMF, Bu_4NBr, 110 °C, 10 h.

Scheme 2 Syntheses of **Tr-OFV*n***.

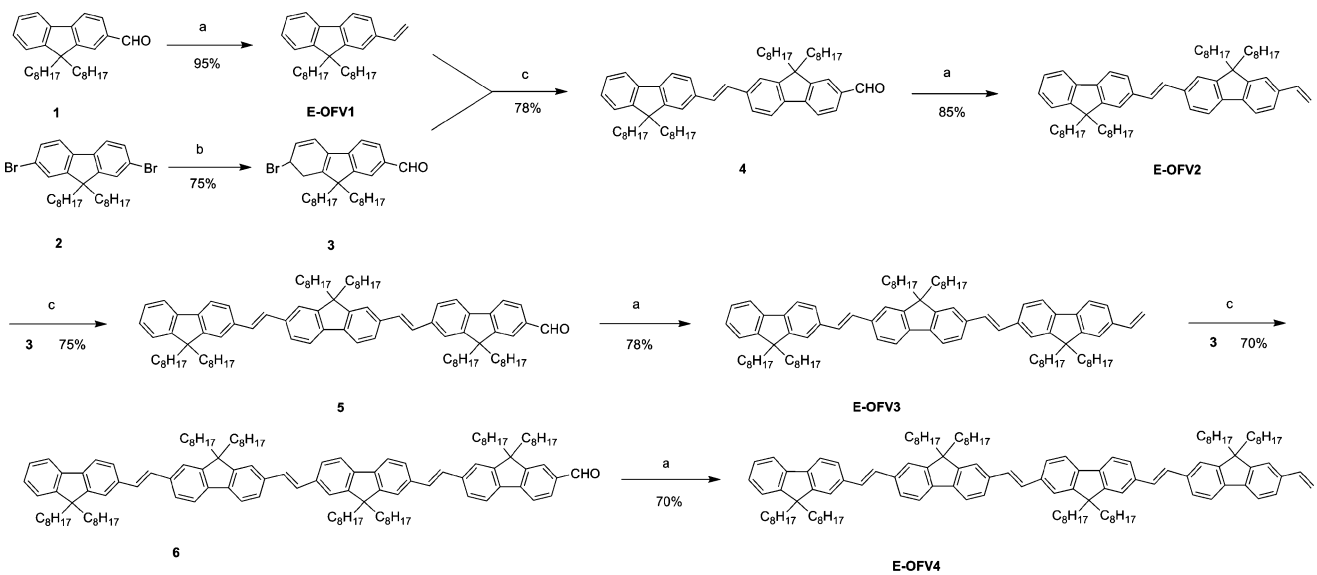

(a) $[Ph_3PCH_3]^+I^-$, t-BuOK, THF, 0 °C, rt; (b) 1) n-BuLi, THF, -78 °C to rt, 2) DMF, -78 °C to rt; (c) $Pd(OAC)_2$, K_2CO_3, DMF, Bu_4NBr, 110 °C, 10 h.

Scheme 1 Syntheses of ***E*-OFV*n***.

Table 1 Photophysical data and HOMO/LUMO energy levels of **Tr-OFV*n***

	Absorption		Photoluminescence		Energy levels/eV			
Compound	Solution[a]	Film	Solution	Film	Φ_F[b]	HOMO[c]	LUMO[d]	δ_{max}/GM (λ/nm)[e]
Tr-OFV1	361 (shoulder), 377, 399	364 (shoulder), 380, 402	407, 431, 458	412, 437, 462	0.93	–5.26	–2.26	65 (700)
Tr-OFV2	385 (shoulder), 404, 427	388 (shoulder), 406, 430	438, 467, 499	448, 477, 510	0.81	–5.25	–2.46	2590 (760)
Tr-OFV3	394 (shoulder), 416, 439	400 (shoulder), 419, 443	452, 481, 515	461, 489, 526	0.93	–5.24	–2.53	6231 (760)
Tr-OFV4	399 (shoulder), 421, 444	406 (shoulder), 423, 448	458, 488, 522	466, 498, 532	0.90	–5.22	–2.54	8073 (760)

[a] Measured in anhydrous THF (2.0×10^{-6} M). [b] Measured in THF with diphenylanthracene (Φ_F = 0.85 in benzene) as a standard excited at 390 nm. [c] Calculated from cyclic voltammogram measurements in CH_2Cl_2. [d] Calculated from the HOMO level and UV-vis absorption edge. [e] Measured in toluene (5.0×10^{-5} M) against rhodamine B (1.0×10^{-4} M in MeOH) as a standard, 1 GM = 10^{-50} cm^4 s $molecule^{-1}$ $photon^{-1}$.

alkylation reaction in a yield of 98%. Then, compound **9** could be prepared by bromination reaction with bromine catalyzed by $FeCl_3$. Finally, the star-shaped macromolecules **Tr-OFV*n*** (n = 1, 2, 3, 4) were synthesized by Heck reaction between ***E*-OFV*n*** and **9**, and the yields for **Tr-OFV1**, **Tr- OFV2**, **Tr-OFV3** and **Tr-OFV4** were 45%, 50%, 51%, and 54%, respectively. All the intermediates and the target molecules were purified by column chromatography, and the new compounds were characterized with FT-IR, ^{1}H NMR, ^{13}C NMR, elemental analysis, and MALDI/TOF mass spectroscopy. **Tr-OFV*n*** exhibited an IR absorption band around 960 cm^{-1} arising from the wagging vibration of the *trans*-double bond (CH═CH).[19] In addition, the ^{1}H NMR spectra of the **Tr-OFV*n*** also confirmed that all the ethenyl groups adopted the *trans*-conformation on account of the absence of a signal at ~6.5 ppm assigned to protons in *cis*-double bonds (CH═CH).[19,20] Due to the introduction of long carbon chains, **Tr-OFV*n*** were readily dissolved in many organic solvents, including dichloromethane, chloroform, toluene, ethyl acetate, and tetrahydrofuran, *etc.*

Photophysical properties

The absorption and photoluminescence spectra of **Tr-OFV*n*** in THF (2.0×10^{-6} M) are shown in Fig. 1, and the photophysical data are listed in Table 1. **Tr-OFV1** gave two distinctive absorption peaks located at 399 nm and 377 nm with a shoulder at 361 nm. With increasing number of fluorene-vinylene units, the absorption bands red-shifted significantly on account of the extending of π-conjugation. For instance, the absorption maximum shifted to 427, 439 and 444 nm for **Tr-OFV2**, **Tr-OFV3** and **Tr-OFV4**, respectively. It suggested that the increase of the number of fluorene-vinylene units could result in the decrease of energy gap (E_g) due to the enlarged conjugation of the oligomers, and the HOMO–LUMO energy gaps (ΔE_{gap}^{opt}) were 3.00 eV, 2.79 eV, 2.71 eV and 2.68 eV for **Tr-OFV1**, **Tr-OFV2**, **Tr-OFV3**, and **Tr-OFV4**, respectively. In addition, from Fig. 1b we could find

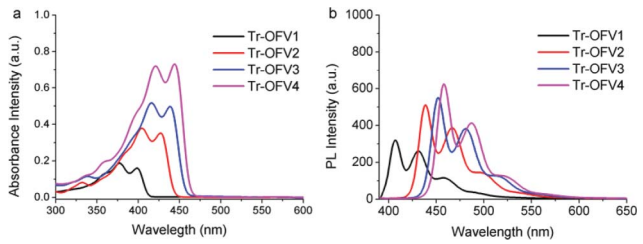

Fig. 1 (a) UV-vis absorption and (b) fluorescence spectra (λ_{ex} = 390 nm) of **Tr-OFV*n*** in THF (2.0×10^{-6} M).

that the fluorescent emission peaks of **Tr-OFV*n*** located at 390–600 nm exhibited typical vibronic structure for polyfluorenes, and they were also red-shifted with increasing length of the arms. The maximal emission band red-shifted from 407 nm for **Tr-OFV1** to 458 nm for **Tr-OFV4**. Moreover, it should be noted that the oligomers **Tr-OFV*n*** are highly emissive, and the fluorescence quantum yields (Φ_F) in THF were in the range of 0.81–0.93 against diphenylanthracene as a standard.

Fig. 2 shows the absorption and emission spectra of **Tr-OFV*n*** (n = 1, 2, 3, 4) in the films obtained *via* spinning the toluene solutions (10 mg mL^{-1}) onto quartz slides. Similarly, the absorption and fluorescence bands red-shifted with increasing the number of fluorene-vinylene units because of the enhanced conjugation. In addition, in comparison with the ones in solutions, **Tr-OFV*n*** showed a red-shift of 5–10 nm of the absorption and emission bands. For example, the absorption maximum of **Tr-OFV3** in the film red-shifted to 443 nm from 439 nm in the solution, indicating the occurrence of the intermolecular interaction in the solid state. In addition, if the spin-coated films were thermally annealed, the absorption bands of **Tr-OFV*n*** became broad without shift, while the emission peaks were broadened accompanied with slight red-shift (Fig. S2†), suggesting that the molecules would be further organized in the thermally annealed films.

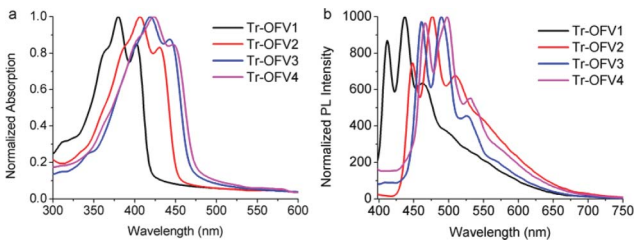

Fig. 2 Normalized (a) UV-vis absorption and (b) fluorescence spectra (λ_{ex} = 390 nm) of **Tr-OFV*n*** in the film.

Electrochemical properties

The cyclic voltammetry (CV) diagrams of **Tr-OFV*n*** (n = 1, 2, 3, 4) in methylene chloride (DCM) in the presence of Bu_4NBF_4 as the supporting electrolyte are shown in Fig. S1† using platinum button as the working electrode, a platinum wire as the counter electrode and Ag/AgCl as the reference electrode under N_2 atmosphere. The redox potential of Fc/Fc^+, which possesses an absolute energy level of –4.8 eV relative to the vacuum level for calibration, is located at 0.37 eV in 0.10 M Bu_4NBF_4/DCM solution at a scan

rate of 100 mV s^{-1}. Therefore, the evaluation of the HOMO and LUMO energy levels could be made according to the following equations:

$$\text{HOMO (eV)} = -E_{ox} - 4.43 \quad (1)$$

$$\text{LUMO (eV)} = -E_{red} - 4.43 \quad (2)$$

where E_{ox} and E_{red} are the measured potentials relative to the standard calomel electrode (SCE). As a result, the HOMO energy levels were of −5.26 eV, −5.25 eV, −5.24 eV and −5.22 eV for **Tr-OFV1**, **Tr-OFV2**, **Tr-OFV3**, and **Tr-OFV4**, respectively. It suggested that the electron-donating ability would be enhanced with increasing the length of the arms based on fluorene-vinylene units.

Two-photon absorption and two-photon emission

The two-photon absorption properties of the star-shaped macromolecules **Tr-OFV*n*** have been studied by femtosecond pulsed laser experiments in toluene at a concentration of 5.0×10^{-5} M. The TPA cross sections have been determined by the two-photon fluorescence method.[21] Herein, **Tr-OFV3** was selected as an example, as shown in Fig. 3; it was interesting that the output intensity of two-photon excited fluorescence emission was linearly dependent on the square of the input laser intensity, thereby confirming the nonlinear absorption of **Tr-OFV3**, which is not a typical TPA compound because of the absence of strong donor and acceptor units. Moreover, the single-photon-induced and two-photon-induced fluorescence spectra overlapped with each other (Fig. 4 and Fig. S3†), suggesting that the emission occurred from the same excited states, regardless of the mode of excitation. Comparing the one-photon absorption and two-photon excitation spectra as shown in Fig. 4, it was clear that the two-photon-allowed state of **Tr-OFV3** was located at somewhat higher energy than that of one-photon allowed states.[22] Nevertheless, there was a significant overlap between one- and two-photon spectra in terms of the total absorption energy, indicating that **Tr-OFV3** might show a large two-photon absorption cross section.[23] As to the oligomers **Tr-OFV1**, **Tr-OFV2** and **Tr-OFV4**, the one- and two-photon spectra could also overlap reasonably in terms of the total absorption energy (Fig. S4†).

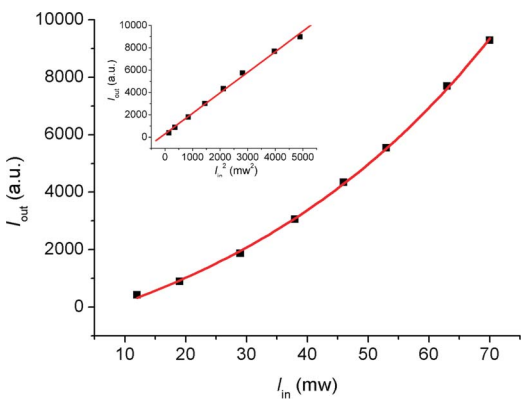

Fig. 3 Dependence of the output fluorescence intensity (I_{out}) of **Tr-OFV3** in toluene on the input laser power (I_{in}). The insert shows the linear dependence of I_{out} on I_{in}^2 (λ_{em} = 710 nm).

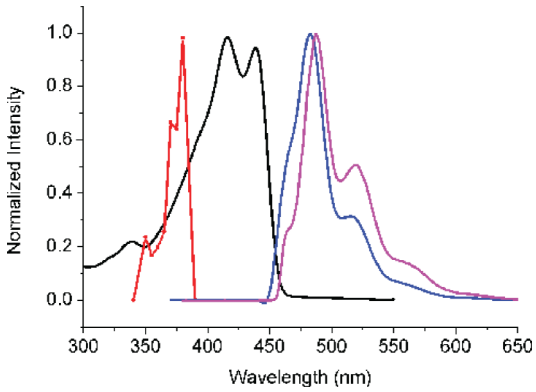

Fig. 4 Normalized one-photon absorption (black), two-photon excitation spectra (red), single-photo-induced fluorescence (blue, λ_{ex} = 365 nm) and two-photon-induced fluorescence spectra (purple, λ_{ex} = 710 nm) of **Tr-OFV3** in toluene (5.0×10^{-5} M). The two-photon excitation spectrum is plotted against $\lambda/2$ (twice the photon energy).

Fig. 5 gives the two-photon-induced fluorescence excitation spectra of **Tr-OFV*n*** (n = 1, 2, 3, 4) in toluene. All compounds showed modest to large two-photon cross sections ranging from 65 to 8073 GM at around 760 nm (Table 1) although no strong donor and acceptor units were involved in the star-shaped **Tr-OFV*n***. It was clear that the δ_{max} value increased with the increasing number of fluorine-vinylene units, and it reached 8073 GM for **Tr-OFV4**, which made it one of the most competitive compounds with enhanced TPA cross section. The arms of fluorine-vinylene seemed to stabilize the excited state more than the ground state to diminish the energy gap between the ground and two-photon-allowed states.[22] As the conjugation was extended with prolonging the arms in **Tr-OFV*n***, the E_g would decrease and the density of states would increase, which may provide more effective coupling channels between the ground and two-photon-allowed states. Therefore, the smaller was the energy gap, the higher was the probability of the two-photon excitation.[24] Moreover, in order to reveal the effect of the star-shaped configuration of **Tr-OFV*n*** on their TPA properties, we investigated the two-photon excitation spectra of the arms of ***E*-OFV*n*** (n = 1, 2, 3, 4) in toluene. It was found that ***E*-OFV1** did not show TPA activity, and the TPA cross sections were 260, 215 and 597 GM for ***E*-OFV2**, ***E*-OFV3** and ***E*-OFV4**, respectively (Fig. S5†), which were quite lower than those

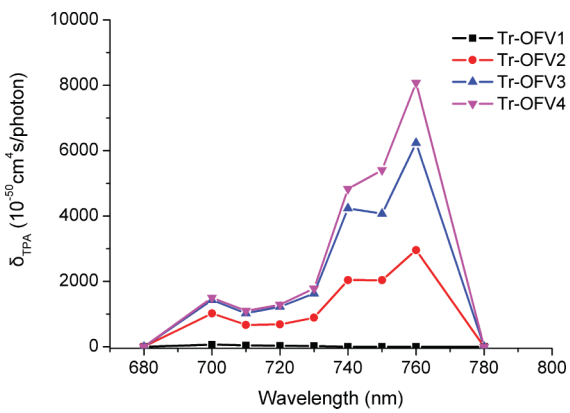

Fig. 5 Two-photon excitation spectra of **Tr-OFV*n*** in toluene (5.0×10^{-5} M).

of the corresponding star-shaped macromolecules **Tr-OFV*n*** (n = 2, 3, 4). For instance, the TPA cross section of **Tr-OFV4** was more than 13 times higher than that of ***E*-OFV4**. As a result, the TPA cross sections could be enhanced significantly when ***E*-OFV*n*** were linked by truxene to afford star-shaped molecules. It illustrated that the branched star-shaped configuration was important for the high TPA cross sections of **Tr-OFV*n*** without strong donor and acceptor units, which would be helpful for designing functional molecules with larger two-photon cross sections.

Conclusions

In summary, we have synthesized a series of new well-defined, monodisperse, star-shaped oligo(9,9-di-n-octylfluorene-2,7-vinylene)s functionalized truxenes **Tr-OFV*n*** (n = 1, 2, 3, 4) by alternate Heck and Wittig reactions. The one-photon absorption and single-photon-induced emission red-shifted with increasing the number of fluorene-vinylene units because of the enlargement of the conjugation. It was interesting that the conjugated oligomers without strong donor and acceptor units exhibited two-photon absorption properties. The δ_{max} values increased obviously with prolonging the arms, and it reached 8073 GM for **Tr-OFV4**, which was one of the highest δ_{max} values reported. It suggested that the low E_g, which could be tuned by the molecular conjugation, was of importance in realising effective coupling channels between the ground and two-photon-allowed states. Meanwhile, the branched star-shaped configuration also favored for the high TPA cross sections of **Tr-OFVn**. As a result, the obtained monodisperse oligomers may find applications in photonics, such as optical power limiting, optical data storage, and so on. Notably, a new platform for exploiting strong TPA compounds was achieved based on the extended π-conjugated systems without strong donor and acceptor units.

Experimental section

Materials and measurements

^{1}H NMR spectra were recorded on a Mercury plus 500 MHz using $CDCl_3$ as solvent in all cases. ^{13}C NMR spectra were recorded on a Mercury plus 125 MHz using $CDCl_3$ as solvent in all cases. UV-vis spectra were determined on a Shimadzu UV-1601PC spectrophotometer. Photoluminescence (PL) spectra were carried out on a Shimadzu RF-5301 luminescence spectrometer. IR spectra were measured using a Germany Bruker Vertex 80v FT-IR spectrometer by incorporating samples in KBr disks. Mass spectra were performed on Agilent 1100 MS series and AXIMA CFR MALDI/TOF (Matrix assisted laser desorption ionization/Time-of-flight) MS (COMPACT). C, H and N elemental analyses were taken on a Perkin-Elmer 240C elemental analyzer. Cyclic voltammetry (CV) was performed using BASIEpsilon workstation and measurements were carried out in DCM containing 0.1 M Bu_4NBF_4 as a supporting electrolyte. Platinum button was used as a working electrode and a platinum wire as a counter electrode; all potentials were recorded *versus* Ag/AgCl (saturated) as a reference electrode. The scan rate was maintained at 100 mV s^{-1}. The two-photon cross section was determined by using a femtosecond (fs) fluorescence measurement technique as described below.[23] The two-photon-induced fluorescence intensities of **Tr-OFV*n*** in toluene (5.0×10^{-5} M) were measured at 680–800 nm by using rhodamine B (1.0×10^{-4} M) as the reference. The intensities of the two-photon-induced fluorescence spectra of the reference and the samples emitted at the same excitation wavelength were recorded. The TPA cross section was calculated according to the following equation,

$$\delta_s = \frac{S_s \eta_r \phi_r N_r}{S_r \eta_s \phi_s N_s} \delta_r$$

where the subscripts s and r stand for the sample and reference molecules, S is the intensity of observed two-photon-induced fluorescence signal, η is the fluorescence quantum yield, N is the concentration of the chromophore, and Φ is the collection efficiency of the experimental setup, δ_r is the TPA cross section of the reference molecule. Ether and tetrahydrofuran (THF) were distilled over sodium and benzophenone. DMF was distilled from phosphorous pentoxide, and other chemicals were used as received without further purification.

Synthetic procedures and characterizations

2-Formyl-9,9-di-n-octylfluorene (**1**), 2,7-dibromo-9,9-di-n-octylfluorene (**2**), 2-bromo-7-formyl-9,9-di-n-octylfluorene (**3**) and truxene (**7**) were synthesized following ref. 9a, 12, 25.

2-Ethenyl-9,9-di-n-octylfluorene (*E*-OFV1). Potassium *tert*-butoxide 2.60 g (23.2 mmol) was added to a solution of 11.6 g (28.6 mmol) triphenylmethylphosphonium iodine in 50 mL dry THF. After the reaction mixture was stirred at room temperature for 15 min, 8.00 g 2-formyl-9,9-di-n-octylfluorene (**1**) (19.1 mmol) was added at 0 °C. Then, the mixture was stirred at room temperature for another 3 h, then poured into 400 mL water. The mixture was extracted with CH_2Cl_2 (3 × 50 mL), the organic liquid was collected and washed with brine, and then dried with anhydrous magnesium sulfate. After the solvent was removed, the crude product was purified by column chromatography (silica gel) with petroleum ether as eluent to afford 7.56 g (95%) of ***E*-OFV1** as a colorless oil. ^{1}H NMR (500 MHz, $CDCl_3$) δ = 7.65 (dd, J = 10.9, 6.9 Hz, 2H), 7.38 (dd, J = 13.1 Hz, 6.4, 2H), 7.35–7.25 (m, 3H), 6.87–6.74 (m, 1H), 5.80 (d, J = 17.5 Hz, 1H), 5.26 (d, J = 10.8 Hz, 1H), 2.10–1.96 (m, 4H), 1.23–1.01 (m, 20H), 0.86–0.77 (m, 6H), 0.62 (s, 4H) (Fig. S6†). IR (KBr, cm^{-1}): 2928, 2854, 1697, 1606, 1466, 1455, 831, 740. Elemental analysis calculated for $C_{31}H_{44}$: C, 89.36; H, 10.64. Found: C, 89.45; H, 10.54. MS, m/z: cal: 416.7, found: 416.6 (Fig. S7†).

(*E*)-7-(2-(9,9-Dioctyl-9*H*-fluoren-2-yl)vinyl)-9,9-dioctyl-9*H*-fluorene-2-carbaldehyde (4). A mixture of 2.00 g (4.80 mmol) of 2-ethenyl-9,9-di-n-octylfluorene (***E*-OFV1**), 2.30 g (4.62 mmol) 2-bromo-7-formyl-9,9-di-n-octylfluorene (**3**), 1.30 g (9.42 mmol) anhydrous potassium carbonate, 1.50 g (4.65 mmol) tetrabutylammonium bromide, and 20 mg (0.089 mmol) $Pd(OAc)_2$ was added into 12 mL anhydrous DMF under N_2 atmosphere. The mixture was stirred at 110 °C for 12 h and then was cooled to room temperature. After being poured into 400 mL water with stirring, the mixture was extracted with CH_2Cl_2 (3 × 50 mL). The organic liquid was washed with brine, and then dried with anhydrous $MgSO_4$. The solvent was removed and the crude product was purified on silica gel column chromatography with petroleum ether/dichloromethane (v/v = 7/2) as eluent,

followed by recrystallization in a THF/ethanol mixture to give a light green solid in yield of 3.11 g, 78%. Mp: 102.0–104.0 °C. IR: ^{1}H NMR (500 MHz, $CDCl_3$) δ 10.06 (s, 1H), 7.88–7.84 (m, 2H), 7.82 (d, J = 7.7 Hz, 1H), 7.77 (d, J = 7.9 Hz, 1H), 7.70 (d, J = 7.6 Hz, 2H), 7.58 (d, J = 8.0 Hz, 1H), 7.56–7.52 (m, 3H), 7.32 (ddd, J = 14.2, 11.4, 6.8 Hz, 5H), 2.08–1.96 (m, 8H), 1.20–1.01 (m, 40H), 0.85–0.76 (m, 12H), 0.68–0.54 (m, 8H) (Fig. S8†). IR (KBr, cm^{-1}): 2922, 2852, 1694, 1603, 1466, 1206, 1156, 966, 822, 740. Elemental analysis calculated for $C_{61}H_{84}O$: C, 87.92; H, 10.16; O, 1.92. Found: C, 87.97; H, 10.10. MS, *m/z*: cal: 833.3, found: 833.1 (Fig. S9).

(*E*)-2-(2-(9,9-Dioctyl-9*H*-fluoren-2-yl)vinyl)-9,9-dioctyl-7-vinyl-9*H*-fluorene (*E*-OFV2). ***E*-OFV2** was prepared from compound **4** following the similar procedure as ***E*-OFV1** in a yield of 85% as a pale blue solid. Mp: 92.0–94.0 °C. ^{1}H NMR (500 MHz, $CDCl_3$) δ 7.71–7.62 (m, 4H), 7.52 (dd, J = 9.0, 7.0 Hz, 4H), 7.42–7.27 (m, 6H), 7.25 (s, 1H), 6.81 (dd, J = 17.6, 10.9 Hz, 1H), 5.81 (d, J = 17.6 Hz, 1H), 5.26 (d, J = 11.0 Hz, 1H), 2.04–1.96 (m, 8H), 1.21–1.03 (m, 40H), 0.85–0.74 (m, 12H), 0.64 (s, 8H) (Fig. S10†). IR (KBr, cm^{-1}): 2924, 2852, 1628, 1606, 1468, 1376, 1211, 966, 888, 823, 740. Elemental analysis calculated for $C_{62}H_{86}$: C, 89.57; H, 10.43. Found: C, 89.46 H, 10.30; MS, *m/z*: cal: 831.3, found: 831.2 (Fig. S11).

7-((*E*)-2-(7-((*E*)-2-(9,9-Dioctyl-9*H*-fluoren-2-yl)vinyl)-9,9-dioctyl-9*H*-fluoren-2-yl)vinyl)-9,9-dioctyl-9*H*-fluorene-2-carbaldehyde (5). Compound **5** was prepared from ***E*-OFV2** and 2-bromo-7-formyl-9,9-di-n-octylfluorene (**3**) following the general procedure for **4** in a yield of 75% as a light yellow solid. Mp: 74.0–76.0 °C. ^{1}H NMR (500 MHz, $CDCl_3$) δ 10.06 (s, 1H), 7.89–7.81 (m, 3H), 7.76 (s, 1H), 7.69 (d, J = 7.5 Hz, 4H), 7.59 (d, J = 7.8 Hz, 1H), 7.56–7.51 (m, 7H), 7.35–7.27 (m, 7H), 2.08–1.98 (m, 12H), 1.23–1.01 (m, 60H), 0.83–0.75 (m, 18H), 0.71–0.57 (m, 12H) (Fig. S12†). IR (KBr, cm^{-1}): 2925, 2853, 1695, 1603, 1466, 1204, 1155, 963, 824, 740. Elemental analysis calculated for $C_{92}H_{126}O$: C, 88.54; H, 10.18; O, 1.28. Found: C, 88.62, H, 10.07. MS, *m/z*: cal: 1247.9, found: 1247.6 (Fig. S13).

2-((*E*)-2-(9,9-Dioctyl-7-vinyl-9*H*-fluoren-2-yl)vinyl)-7-((*E*)-2-(9,9-dioctyl-9*H*-fluoren-2-yl)vinyl)-9,9-dioctyl-9*H*-fluorene (*E*-OFV3). ***E*-OFV3** was prepared from compound **5** following the similar procedure as for ***E*-OFV1** in a yield of 78% as a yellow solid. Mp: 76.0–78.0 °C. ^{1}H NMR (500 MHz, $CDCl_3$) δ = 7.68 (dd, J = 12.8, 6.0, 5H), 7.64 (d, J = 7.8, 1H), 7.53 (d, J = 12.7, 8H), 7.35 (ddd, J = 19.9, 15.1, 7.7, 5H), 7.28 (s, 4H), 6.81 (dd, J = 17.5, 10.9, 1H), 5.81 (d, J = 17.6, 1H), 5.26 (d, J = 10.9, 1H), 2.06–1.98 (m, 12H), 1.21–1.04 (m, 60H), 0.85–0.75 (m, 18H), 0.70–0.62 (m, 12H) (Fig. S14†). IR (KBr, cm^{-1}): 2926, 2853, 1628, 1606, 1467, 1377, 1207, 961, 823, 740. Elemental analysis calculated for $C_{93}H_{128}$: C, 89.65; H, 10.35. Found: C, 89.58, H, 10.27. MS, *m/z*: cal: 1246.0, found: 1245.5 (Fig. S15†).

7-((*E*)-2-(7-((*E*)-2-(7-((*E*)-2-(9,9-Dioctyl-9*H*-fluoren-2-yl)vinyl)-9,9-dioctyl-9*H*-fluoren-2-yl)vinyl)-9,9-dioctyl-9*H*-fluoren-2-yl)vinyl)-9,9-dioctyl-9*H*-fluorene-2-carbaldehyde (6). Compound **6** was prepared from ***E*-OFV3** and 2-bromo-7-formyl-9,9-di-n-octylfluorene (**3**) following the general procedure for **4** in a yield of 70% as a yellow solid. Mp: 64.0–66.0 °C. ^{1}H NMR (500 MHz, $CDCl_3$) δ = 10.07 (s, 1H), 7.85 (dd, J = 21.6, 9.8, 3H), 7.78 (d, J = 7.8, 1H), 7.69 (d, J = 7.5, 6H), 7.57 (dd, J = 25.5, 11.0, 12H), 7.37–7.26 (m, 9H), 2.11–1.97 (m, 16H), 1.21–1.01 (m, 80H), 0.90–0.71 (m, 24H), 0.67 (s, 16H) (Fig. S16†). IR (KBr, cm^{-1}): 2925, 2853, 1695, 1603, 1466, 1204, 1155, 962, 823, 740. Elemental analysis calculated for $C_{123}H_{168}O$: C, 88.85; H, 10.18; O, 0.96. Found: C, 88.78, H, 10.11. MS, *m/z*: cal: 1662.6, found: 1662.1 (Fig. S17).

2-((*E*)-2-(9,9-Dioctyl-7-vinyl-9*H*-fluoren-2-yl)vinyl)-7-((*E*)-2-(7-((*E*)-2-(9,9-dioctyl-9*H*-fluoren-2-yl)vinyl)-9,9-dioctyl-9*H*-fluoren-2-yl)vinyl)-9,9-dioctyl-9*H*-fluorene (*E*-OFV4). ***E*-OFV4** was prepared from compound **6** following the similar procedure as for ***E*-OFV1** in a yield of 70% as a yellow solid. Mp: 68.0–70.0 °C. ^{1}H NMR (500 MHz, $CDCl_3$) δ = 7.74–7.60 (m, 8H), 7.54 (d, J = 12.4, 12H), 7.43–7.26 (m, 11H), 6.81 (dd, J = 17.5, 10.9, 1H), 5.81 (d, J = 17.6, 1H), 5.26 (d, J = 10.9, 1H), 2.08–1.97 (m, 16H), 1.21–1.04 (m, 80H), 0.86–0.74 (m, 24H), 0.67 (s, 16H) (Fig. S18†). IR (KBr, cm^{-1}): 2924, 2852, 1627, 1607, 1467, 1376, 1208, 965, 823, 738. Elemental analysis calculated for $C_{124}H_{170}$: C, 89.68; H, 10.32. Found: C, 89.61, H, 10.25. MS, *m/z*: cal: 1660.7, found: 1659.8 (Fig. S19).

5,5,10,10,15,15-Hexabutyl-truxene (8)

With vigorous stirring, 30.3 mL of n-BuLi (1.93 M, 58.48 mmol) was added to a suspension of truxene (2.00 g, 5.84 mmol) in 60 mL of anhydrous ethyl ether at −78 °C and the mixture was kept at this temperature over a period of 2 h. A solution of n-butyl bromide (8.00 g, 58.39 mmol) was then added dropwise. The reaction mixture was allowed to warm to room temperature slowly and stirred overnight. The mixture was then poured into 200 mL of saturated aqueous NaCl solution with stirring for 15 min. The water phase was extracted with ethyl acetate twice, and then the combined organic phase was dried over $MgSO_4$. After the solvent was removed, the residue was purified by flash column chromatography (silica gel) using petroleum ether as eluent to afford a light yellow solid of 5,5,10,10,15,15-hexabutyl-truxene (3.91 g, 98%). Mp: 230.0–232.0 °C. ^{1}H NMR (500 MHz, $CDCl_3$) δ 8.38 (d, J = 7.6 Hz, 3H), 7.47 –7.46 (m, 3H), 7.42–7.34 (m, 6H), 3.01–2.95 (m, 6H), 2.13–2.07 (m, 6H), 0.93–0.84 (m, 12H), 0.56–0.42 (m, 30H). (Fig. S20†). IR (KBr, cm^{-1}): 2955, 2927, 2870, 2857, 1470, 1455, 1376, 1366, 1160, 1036, 905, 892, 746. Elemental analysis calculated for $C_{51}H_{66}$: C, 90.20; H, 9.80. Found: C, 90.12; H, 9.86. MS, *m/z*: cal: 679.0, found: 768.4 (Fig. S21).

5,5,10,10,15,15-Hexabutyl-2,7,12-tribromotruxene (9)

To a mixture of **8** (3.00 g, 4.12 mmol) and 20 mg of anhydrous $FeCl_3$ as catalyst in 60 mL chloroform, a solution of bromine (0.82 mL, 16.00 mmol) in 10 mL chloroform was added dropwise at 0 °C over 1 h. After stirring at 0 °C for 24 h, the mixture was washed with saturated sodium thiosulfate solution and brine to remove excess bromine. The precipitate was filtered and washed with water three times. The organic phase was washed with brine. After removal of the solvent a solid residue was afforded. The crude product was recrystallized from EtOH to yield a white solid of compound **9** (3.84 g, 95%). Mp: > 230.0 °C. ^{1}H NMR (500 MHz, $CDCl_3$) δ 8.19 (d, J = 8.5 Hz, 3H), 7.57 (s, 3H), 7.52 (d, J = 8.2 Hz, 3H), 2.93–2.80 (m, 6H), 2.10–1.98 (m, 6H), 0.94–0.84 (m, 12H), 0.56–0.36 (m, 30H). (Fig. S22†). IR (KBr, cm^{-1}): 2955, 2926, 2870, 2858, 1590, 1468, 1455, 1377, 1358, 1179, 1078, 905, 881, 832, 800, 754,

727. Elemental analysis calculated for $C_{51}H_{63}Br_3$: C, 66,89; H, 6.93; Br, 26.18. Found: C, 66.97; H, 6.89.

Tr-OFV1

A mixture of 2-ethenyl-9,9-di-n-octylfluorene (***E*-OFV1**, 2.00 g, 4.8 mmol), 5,5,10,10,15,15-hexabutyl-2,7,12-tribromotruxene (0.70 g, 0.76 mmol), anhydrous potassium carbonate (0.63 g, 4.56 mmol), tetrabutylammonium bromide (0.74 g, 2.28 mmol), and $Pd(OAc)_2$ (20 mg, 0.089 mmol) was added into 10 mL anhydrous DMF under N_2 atmosphere. The mixture was stirred at 110 °C for 12 h and then was cooled to room temperature. After being poured into 400 mL water with stirring, the mixture was extracted with CH_2Cl_2 (3 × 30 mL). The organic liquid was washed with brine and then dried with anhydrous $MgSO_4$. After the solvent was removed, the crude product was purified by column chromatography (silica gel) with petroleum ether/dichloromethane (v/v = 40/1) as eluent to give a light blue solid (0.65 g, 45%). Mp: 79.0–81.0 °C. ^{1}H NMR (500 MHz, $CDCl_3$) δ 8.43 (d, J = 8.5 Hz, 3H), 7.81–7.74 (m, 6H), 7.67 (d, J = 6.8 Hz, 6H), 7.61 (d, J = 9.4 Hz, 6H), 7.43–7.31 (m, 15H), 3.14–2.97 (m, 6H), 2.27–2.14 (m, 6H), 2.10–2.00 (m, 12H), 1.29–1.10 (m, 60H), 1.02–0.93 (m, 12H), 0.85 (m, 18H), 0.70 (m, 18H), 0.52 (m, 24H) (See Figure S23†). ^{13}C NMR (125 MHz,$CDCl_3$) δ 154.62, 151.69, 151.41, 145.65, 141.31, 140.43, 138.67, 136.93, 136.12, 129.37, 128.65, 127.43, 127.20, 126.06, 125.34, 125.08, 123.27, 121.09, 120.57, 120.32, 120.07, 56.03, 55.45, 40.93, 37.28, 32.22, 30.50, 29.65, 27.02, 24.19, 23.32, 23.01, 14.48, 14.28 (Fig. S24†). IR (KBr, cm^{-1}): 2957, 2924, 2852, 1466, 1456, 1375, 1338, 1116, 961, 886, 833, 739. Elemental analysis calculated for $C_{144}H_{192}$: C, 89.94; H, 10.06. Found: C, 90.12, H, 9.89. MS, m/z: cal: 1923.1, found: 1922.3 (Fig. S25).

Tr-OFV2

Tr-OFV2 was prepared from 5,5,10,10,15,15-hexabutyl-2,7,12-tribromotruxene and ***E*-OFV2** following the general procedure for **Tr-OFV1** in a yield of 50% as a yellowish solid. Mp: 101.0–103.0 °C.^{1}H NMR (500 MHz, $CDCl_3$) δ 8.41 (d, J = 8.5 Hz, 3H), 7.72–7.69 (m, 12H), 7.65 (d, J = 7.0 Hz, 6H), 7.60–7.53 (m, 18H), 7.39–7.26 (m, 21H), 3.05 (s, 6H), 2.19 (s, 6H), 2.07–1.99 (m, 24H), 1.22–1.07 (m, 120H), 0.99–0.90 (m, 12H), 0.83–0.80 (m, 36H), 0.74–0.60 (m, 30H), 0.56–0.44 (m, 24H) (Fig. S26†). ^{13}C NMR (125 MHz, $CDCl_3$) δ 154.63, 151.98, 151.67, 151.38, 145.68, 141.29, 141.10, 140.45, 138.68, 136.95, 136.13, 129.36, 128.97, 128.69, 127.41, 127.19, 126.13, 126.00, 125.35, 125.11, 123.26, 121.03, 120.58, 120.32, 120.05, 56.04, 55.44, 41.09, 40.94, 37.28, 32.22, 30.50, 29.66, 27.02, 24.18, 23.33, 23.01, 14.47, 14.28 (Fig. S27†). IR (KBr, cm^{-1}): 2955, 2925, 2854, 1466, 1456, 1375, 1338, 1202, 1116, 961, 884, 830, 739. Elemental analysis calculated for $C_{237}H_{318}$: C, 89.88; H, 10.12. Found: C, 89.96; H, 10.01. MS, m/z: cal: 3167.06, found: 3167.4 (Fig. S28).

Tr-OFV3

Tr-OFV3 was prepared from 5,5,10,10,15,15-hexabutyl-2,7,12-tribromotruxene and ***E*-OFV3** following the general procedure for **Tr-OFV1** in a yield of 51% as a light yellow solid. Mp: 121.0–123.0 °C. ^{1}H NMR (500 MHz, $CDCl_3$) δ 8.41 (s, 3H), 7.74–7.68 (m, 18H), 7.67 (s, 6H), 7.61–7.52 (m, 30H), 7.39–7.27 (m, 27H), 3.05 (s, 6H), 2.20 (s, 6H), 2.12–1.97 (m, 36H), 1.26–1.01 (m, 180H), 1.01–0.92 (m, 12H), 0.85–0.77 (m, 54H), 0.75–0.63 (m, 42H), 0.56–0.47 (m, 24H) (Fig. S29†). ^{13}C NMR (125 MHz, $CDCl_3$) δ 154.63, 151.96, 151.67, 151.37, 145.68, 141.29, 141.06, 140.45, 138.68, 136.93, 136.13, 129.35, 129.02, 128.70, 127.41, 127.19, 126.12, 126.00, 125.36, 125.12, 123.25, 121.02, 120.31, 120.55, 120.05, 56.04, 55.45, 41.11, 40.95, 37.30, 32.22, 30.52, 29.67, 27.04, 24.19, 23.33, 23.01, 14.47, 14.29 (Fig. S30†). IR (KBr, cm^{-1}): 2955, 2924, 2852, 1466, 1456, 1375, 1337, 1300, 1202, 960, 884, 826, 739. Elemental analysis calculated for $C_{330}H_{444}$: C, 89.85; H, 10.15. Found: C, 89.96; H, 10.02. MS, m/z: cal: 4411.06, found: 4411.5 (Fig. S31).

Tr-OFV4

Tr-OFV4 was prepared from 5,5,10,10,15,15-hexabutyl-2,7,12-tribromotruxene and ***E*-OFV4** following the general procedure for **Tr-OFV1** in a yield of 54% as a light yellow solid. Mp: 147.0–149.0 °C. ^{1}H NMR (500 MHz, $CDCl_3$) δ 8.41 (s, 3H), 7.74–7.68 (m, 24H), 7.67–7.63 (m, 6H), 7.61–7.52 (m, 42H), 7.39–7.27 (m, 33H), 3.05 (s, 6H), 2.19 (s, 6H), 2.12–1.96 (m, 48H), 1.24–1.04 (m, 240H), 0.99–0.91 (m, 12H), 0.85–0.77 (m, 72H), 0.74–0.60 (m, 54H), 0.55–0.44 (m, 24H) (see Fig. S32†). ^{13}C NMR (126 MHz, $CDCl_3$) δ 154.63, 151.96, 151.67, 151.38, 145.68, 141.29, 141.06, 140.47, 138.69, 136.93, 136.13, 129.36, 129.02, 128.69, 127.41, 127.19, 126.13, 126.00, 123.25, 121.01, 120.63, 120.32, 120.05, 56.05, 55.45, 41.11, 40.95, 37.32, 32.22, 30.52, 29.67, 27.05, 24.19, 23.33, 23.01, 14.47, 14.29 (Fig. S33†). IR (KBr, cm^{-1}): 2957, 2925, 2852, 1466, 1456, 1375, 1337, 1300, 1245, 1204, 961, 881, 822, 739. Elemental analysis calculated for $C_{423}H_{570}$: C, 89.84; H, 10.16. Found: C, 90.02; H, 10.25. MS, m/z: cal: 5655.1, found: 5655.6 (Fig. S34).

Acknowledgements

This work is financially supported by the National Natural Science Foundation of China (20874034 and 51073068), 973 Program (2009CB939701) and Open Project of State Key Laboratory of Supramolecular Structure and Materials (SKLSSM200901).

Notes and references

1 (*a*) W. Denk, J. H. Strickler and W. W. Webb, *Science*, 1990, **248**, 73–76; (*b*) L. Ventelon, S. Charier, L. Moreaux, J. Mertz and M. Blanchard-Desce, *Angew. Chem., Int. Ed.*, 2001, **40**, 2098–2101; (*c*) J. Mertz, C. Xu and W. W. Webb, *Opt. Lett.*, 1995, **20**, 2532–2534.

2 (*a*) D. A. Parthenopoulos and P. M. Rentzepis, *Science*, 1989, **245**, 843–845; (*b*) A. S. Dvornikov and P. M. Rentzepis, *Opt. Commun.*, 1995, **119**, 341–346; (*c*) S. Kawata and Y. Kawata, *Chem. Rev.*, 2000, **100**, 1777–1788.

3 (*a*) G. S. He, C. F. Zhao, J. D. Bhawalkar and P. N. Prasad, *Appl. Phys. Lett.*, 1995, **67**, 3703–3705; (*b*) S. L. Oliveira, D. S. Corrêa, L. Misoguti, C. J. L. Constantino, R. F. Aroca, S. C. Zilio and C. R. Mendonça, *Adv. Mater.*, 2005, **17**, 1890–1893.

4 J. D. Bhawalkar, N. D. Kumar, C. F. Zhao and P. N. J. Prasad, *Clin. Laser. Med. Surg.*, 1997, **15**, 201–204.

5 (*a*) C. W. J. Spangler, *J. Mater. Chem.*, 1999, **9**, 2013–2020; (*b*) J. E. Ehrlich, X. L. Wu, I.-Y. S. Lee, Z.-Y. Hu, H. Röckel, S. R. Marder and J. W. Perry, *Opt. Lett.*, 1997, **22**, 1843–1845; (*c*) G. S. He, G. C. Xu, P. N. Prasad, B. A. Reinhardt, J. C. Bhatt and A. G. Dillard, *Opt. Lett.*, 1995, **20**, 435–437; (*d*) X. H. Ouyang, H. P. Zeng and W. J. Ji, *J. Phys. Chem. B*, 2009, **113**, 14565–14573.

6 (*a*) O. Mongin, L. Porrès, M. Charlot, C. Katan and M. Blanchard-Desce, *Chem.–Eur. J.*, 2007, **13**, 1481–1498; (*b*) M. Rumi, J. E. Ehrlich,

A. A. Heikal, J. W. Perry, S. Barlow, Z. Y. Hu, D. McCord-Maughon, T. C. Parker, H. Röckel, S. Thayumanavan, S. R. Marder, D. Beljonne and J.-L. Brédas, *J. Am. Chem. Soc.*, 2000, **122**, 9500–9510; (*c*) G. S. He, L. S. Tan, Q. Zheng and P. N. Prasad, *Chem. Rev.*, 2008, **108**, 1245–1330; (*d*) M. Pawlicki, H. A. Collins, R. G. Denning and H. L. Anderson, *Angew. Chem., Int. Ed.*, 2009, **48**, 3244–3266.
7 (*a*) S.-J. Chung, K.-S. Kim, T.-C. Lin, G. S. He, J. Swiatkiewicz and P. N. Prasad, *J. Phys. Chem. B*, 1999, **103**, 10741–10745; (*b*) G. S. He, J. Swiatkiewicz, Y. Jiang, P. N. Prasad, B. A. Reinhardt, L. S. Tan and R. Kannan, *J. Phys. Chem. A*, 2000, **104**, 4805–4810.
8 (*a*) M. H. V. Werts, S. Gmouh, O. Mongin, T. Pons and M. B. Blanchard-Desce, *J. Am. Chem. Soc.*, 2004, **126**, 16294–16295; (*b*) H. Detert, M. Lehmann and H. Meier, *Materials*, 2010, **3**, 3218–3330.
9 (*a*) X. Y. Cao, X. H. Liu, X. H. Zhou, Y. Zhang, Y. Jiang, Y. Cao, Y. X. Cui and J. Pei, *J. Org. Chem.*, 2004, **69**, 6050–6058; (*b*) X. Y. Cao, W. B. Zhang, J. L. Wang, X. H. Zhou, H. Lu and J. Pei, *J. Am. Chem. Soc.*, 2003, **125**, 12430–12431.
10 (*a*) K. M. Knoblock, C. J. Silvestri and D. M. Collard, *J. Am. Chem. Soc.*, 2006, **128**, 13680–13681; (*b*) T. H. Xu, R. Lu, X. L. Liu, X. Q. Zheng, X. P. Qiu and Y. Y. Zhao, *Org. Lett.*, 2007, **9**, 797–800; (*c*) T. H. Xu, R. Lu, X. L. Liu, P. Chen, X. P. Qiu and Y. Y. Zhao, *Eur. J. Org. Chem.*, 2008, 1065–1071; (*d*) T. H. Xu, R. Lu, X. L. Liu, P. Chen, X. P. Qiu and Y. Y. Zhao, *J. Org. Chem.*, 2008, **73**, 1809–1817; (*e*) X. L. Liu, R. Lu, T. H. Xu, D. F. Xu, Y. Zhan, P. Chen, X. P. Qiu and Y. Y. Zhao, *Eur. J. Org. Chem.*, 2006, **1**, 53–60; (*f*) X. C. Yang, R. Lu, F. Y. Gai, P. C. Xue and Y. Zhan, *Chem. Commun.*, 2010, **46**, 1088–1090; (*g*) S. S. Zade and M. Bendikov, *Org. Lett.*, 2006, **8**, 5243–5246.
11 X. H. Zhou, J. C. Yan and J. Pei, *Org. Lett.*, 2003, **5**, 3543–3546.
12 (*a*) B. S. Li, J. Li, Y. Q. Fu and Z. S. Bo, *J. Am. Chem. Soc.*, 2004, **126**, 3430–3431; (*b*) B. Li, X. Xu, M. Sun, Y. Fu, G. Yu, Y. Liu and Z. S. Bo, *Macromolecules*, 2006, **39**, 456–461.
13 W. Y. Lai, R. Zhu, Q. L. Fan, L. T. Hou, Y. Cao and W. Huang, *Macromolecules*, 2006, **39**, 3707–3709.
14 F. Liu, W. Y. Lai, C. Tang, H. B. Wu, Q. Q. Chen, B. Peng, W. Wei, W. Huang and Y. Cao, *Macromol. Rapid Commun.*, 2008, **29**, 659–664.
15 A. L. Kanibolotsky, R. Berridge, P. J. Skabara, I. F. Perepichka, D. D. C. Bradley and M. Koeberg, *J. Am. Chem. Soc.*, 2004, **126**, 13695–13702.
16 (*a*) H. P. Zhou, R. Lu, X. Zhao, X. P. Qiu, P. C. Xue, X. L. Liu and X. F. Zhang, *Tetrahedron Lett.*, 2010, **51**, 5287–5290; (*b*) M. Todd, W. J. Li and L. P. Yu, *J. Am. Chem. Soc.*, 1997, **119**, 844–845; (*c*) H. F. Heck and J. P. Nolley, *J. Org. Chem.*, 1972, **37**, 2320–2322.
17 X. P. Qiu, R. Lu, H. P. Zhou, X. F. Zhang, T. H. Xu, X. L. Liu and Y. Y. Zhao, *Tetrahedron Lett.*, 2007, **48**, 7582–7585.
18 X. Y. Cao, X. H. Zhou, H. Zi and J. Pei, *Macromolecules*, 2004, **37**, 8874–8882.
19 (*a*) Q. Liu, W. M. Liu, B. Yao, H. K. Tian, Z. Y. Xie, Y. H. Geng and F. S. Wang, *Macromolecules*, 2007, **40**, 1851–1857; (*b*) F. He, H. Xia, S. Tang, Y. Duan, M. Zeng, L. L. Liu, M. Li, H. Q. Zhang, B. Yang, Y. G. Ma, S. Y. Liu and J. C. Shen, *J. Mater. Chem.*, 2004, **14**, 2735–2740.
20 K. Nomura, H. Morimoto, Y. Imanishi, Z. Ramhani and Y. J. Geerts, *J. Polym. Sci., Part A: Polym. Chem.*, 2001, **39**, 2463–2470.
21 F. He, L. L. Tian, X. Y. Tian, H. Xu, Y. H. Wang, W. J. Xie, M. Hanif, J. L. Xia, F. Z. Shen, B. Yang, F. Li, Y. G. Ma, Y. Q. Yang and J. C. Shen, *Adv. Funct. Mater.*, 2007, **17**, 1551–1557.
22 W. M. McClain, *Acc. Chem. Res.*, 1974, **7**, 129–135.
23 S. K. Lee, W. J. Yang, J. J. Choi, C. H. Kim, S.-J. Jeon and B. R. Cho, *Org. Lett.*, 2005, **7**, 323–326.
24 (*a*) B. R. Cho, K. H. Son, S. H. Lee, Y.-S. Song, Y.-K. Lee, S.-J. Jeon, J.-H. Choi, H. Lee and M. Cho, *J. Am. Chem. Soc.*, 2001, **123**, 10039–10045; (*b*) W.-H. Lee, H. Lee, J.-A. Kim, J.-H. Choi, M. Cho, S.-J. Jeon and B. R. Cho, *J. Am. Chem. Soc.*, 2001, **123**, 10658–10667.
25 C. J. Xia and R. C. Advincula, *Macromolecules*, 2001, **34**, 5854–5859.